

Supporting Information

Near-IR absorbing Tetraene-linked π -Conjugated Porous Polymer for Energy Storage and Electrical Conductivity

Vinutha K. Venkatareddy^a, Hamidreza Parsimehr^b, Anna Ignaszak^{*b} and Rajeswara Rao M^{*a}

Contents

1. General information:	2
1.1 General procedure for the synthesis of model compounds (DT-M and DP-M) ³ :.....	3
1.2 General procedure for the synthesis of the DP-P and DT-P polymers <i>via</i> Knoevenagel condensation:.....	4
References:	19

List of figures

Fig S 1: FTIR spectra of compound 1 , 2 , 3 , DT-M , DP-P and DT-P	4
Fig S 2: FTIR spectra of DP-P and DT-P polymers taken after soaking the polymers for 5 days in 1M KOH and 0.5M HCl.	5
Fig S 3: FE-SEM of the DT-P (Left) and DP-P (Right).	5
Fig S 4: TGA of DP-P and DT-P polymers.....	6
Fig S 5: Powder XRD of DP-P and DT-P polymers.	6
Fig S 6: XPS survey scan spectra of DP-P and DT-P polymers.....	7
Fig S 7: High resolution XPS spectra of C 1s (a), N 1s (b), O 1s (c) of DP-P and C 1s (d), N 1s (e), O 1s (f) of DT-P	7
Fig S 8: BET adsorption isotherms of DP-P and DT-P polymers.	8
Fig S 9: The DFT computed frontier molecular orbitals of model compounds DP-M and DT-M (left side) and polymers DP-P and DT-P (right side) by using B3LYP-631G(d) basis set method.....	8
Fig S 10: DFT computed HOCO and LUCO of DT-P polymer.	8
Fig S 11: DFT computed HOCO and LUCO of DP-P polymer.....	9
Fig S 12: Cyclic voltammograms of bare DT-P polymer in 1 KOH recorded at various potential scan rates: 5-100 mV/sec.	14
Fig S 13: A reduction peak current vs. square root of potential scan rate built based on cyclic voltammograms in Fig. S11 for bare DT-P polymer.....	14
Fig S 14: A reduction peak current vs. square root of potential scan rate built based on cyclic voltammograms for DT-P + CB (carbon black).....	15
Fig S 15: The cyclic voltammogram of DT-P polymer (a); DT-P + carbon black (CB) (b); DT-P + CB + graphene oxide (GO) (c).	15
Fig S 16: The cyclic voltammogram of DP-P and DT-P polymers measured by using dichloromethane as solvent and tetrabutylammonium chloride as an electrolyte at 20 mV/s scan rate.	16
Fig S 17: ¹ H NMR of DP-M	16
Fig S 18: ¹³ C NMR of DP-M	17
Fig S 19: ¹ H NMR of DT-M	17
Fig S 20: ¹³ C NMR of DT-M	18

Fig S 21: ¹³ C-CPMAS of DP-P	18
Fig S 22: ¹³ C-CPMAS of DT-P	19

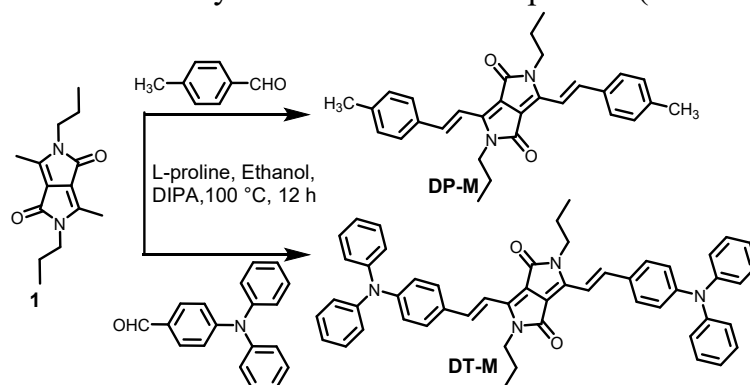
List of tables

Table S 1: Reported active methylene building block.	9
Table S 2: Absorption of the reported DPP integrated 2D polymers.....	11
Table S 3: Electrical conductivity of the reported 2D polymers.....	11
Table S 4: Specific capacitance (C_s ; F/g) and diffusion coefficient (D ; cm ² /s) for bare polymers and their mixture with carbon black (CB) and graphene oxide (GO).....	16

1. General information:

The chemicals and solvents were used without further purification. The chemicals fumaryl chloride, propyl bromide, triethylamine, acetonitrile (ACN), pyridine, *p*-toluene sulfonic acid, isopropenylacetate, dimethylformamide, *p*-tolualdehyde, 4-trifluoromethylbenzaldehyde, ethanol, L-proline, Iodine, Pyridiniumchlorochromate(PCC), LiAlH₄, diethylether, methanol, benzene-1,3,5-tricarboxylic acid, H₂SO₄, Triphenylamine, phosphorousoxychloride, DMF and di-isopropenylamine (DIPA), purchased from suppliers such as Sigma-Aldrich, Tokyo Chemical Industry (TCI), Finar, Loba and Spectrochem. Benzene-1,3,5-tricarbaldehyde (**2**)¹, 4-(diphenylamino)benzaldehyde and 4,4',4''-nitrioltribenzaldehyde (**3**)² were synthesized as per the reported procedure. ¹H-NMR, ¹³C CP-MAS, were measured using JEOL ECZS 400MHz and 100MHz spectrometers. UV-Vis spectra were recorded using the Cary 5000 UV-Vis NIR spectrometer. Electrochemical studies were done by using the Gamry INTERFACE1010 31184 in a three-electrode system, with Pt wire as a counter electrode, Ag/AgCl as a reference electrode, and Glassy carbon as a working electrode. Tetrabutylammonium perchlorate (TBAP) was used as an electrolyte, and HPLC grade dichloromethane as the solvent. Redox potentials were referenced to ferrocene (Fc/Fc⁺). HOMOs were calculated using the equation HOMO = -(4.8 + oxd potential), and LUMOs were determined using LUMO = -(4.8 + Redn potential).

1.1 General procedure for the synthesis of model compounds (**DT-M** and **DP-M**)³:



In a clean and dried RB, the compound **1** (0.4 mmol) in ethanol solvent was added by DIPA (1.61 mmol) followed by L-proline (0.08 mmol) and the corresponding aromatic aldehyde (0.8 mmol). The mixture was stirred at 100 °C for 12 h. The obtained solid was filtered off and washed with diethyl ether followed by hexane to yield the model compounds **DP-M** (Dark purple solid) and **DT-M** (dark green solid) in 85 yields.

Compound **DP-M** (Yields: 85%) HRMS: m/z calculated for C₃₂H₃₄N₂O [M⁺]: 560.1898; found m/z : 560.1901; ¹H NMR (400 MHz, CDCl₃) in δ : 8.93-8.89 (2H, d, J= 16Hz), 7.64-7.75 (8H, dd, J= 8Hz), 6.9-6.94 (2H, d, J= 16Hz), 3.79-3.83 (4H, t), 1.69-1.78 (4H, sextet), 1-1.04 (6H, t); ¹³C-NMR (100 MHz, CDCl₃) δ : 11.6, 23.7, 41.9, 109.8, 115.5, 122.2, 126.0, 128.5, 131.4, 139.3, 141.3, 144.3, 161.6.

Compound **DT-M** (Yields: 85%) HRMS: m/z calculated for C₅₂H₄₆N₄O₂ [M⁺]: 758.3621 ; found m/z : 758.3605; ¹H NMR (400 MHz, CDCl₃) in δ : : 8.79-8.83(2H, d, J= 16 Hz), 7.48-7.50(4H, d, J= 8 Hz), 7.26-7.30 (8H, t), 7.06-7.14 (12H, m), 6.99-7.01(4H, d, J= 8Hz), 6.68-6.72(2H, d, J= 16 Hz), 3.74-3.78 (4H, t), 1.66-1.75(4H, sextet), 0.96-1.0(6H, t) ; ¹³C-NMR (100 MHz, CDCl₃) δ : 11.69, 23.53, 42.16, 108.59, 111.31, 122, 124.14, 125.18, 129.34, 142.60, 144.26, 147.20, 147.3, 149.83, 162.35.

1.2 General procedure for the synthesis of the **DP-P** and **DT-P** polymers *via* Knoevenagel condensation:

The compound **D** (0.12 mmol), trialdehyde (0.08 mmol) and L-proline (0.016 mmol) were taken in a clean and dried pressure vessel was added by a base DIPA (0.32 mmol) and ethanol (4ml) and the mixture was purged for about 15 min by using N₂ gas and then heated at 100 °C for five days to yield dark purple colour solid which was insoluble in highly polar DMF and methanol solvent. The polymer was washed with excess of methanol, dichloromethane followed by DMF to remove the starting material and oligomeric impurities. Further, Soxhlet extraction was done with THF to remove the oligomeric impurities. The obtained insoluble solid was dried under vacuum pump to yield the polymers in 85-90 % yields. **DP-P** (Black solid) and **DT-M** (Black solid): CP-MAS ¹³C: 165 ppm, 150 ppm, 130-140 ppm, 105 ppm, 10 to 50 ppm. FT-IR: 1650 cm⁻¹, 1580 cm⁻¹.

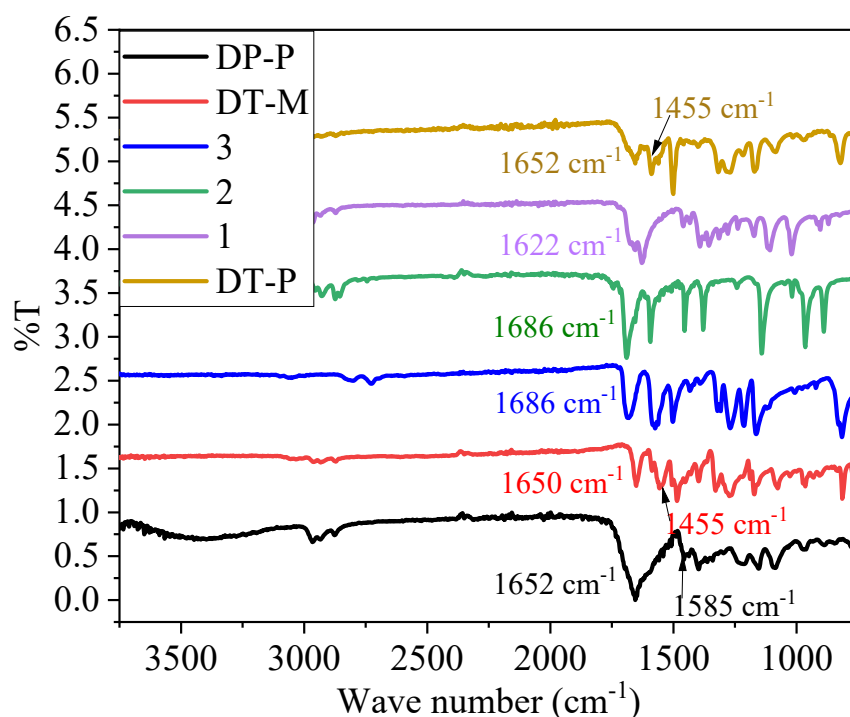


Fig S 1: FTIR spectra of compound **1**, **2**, **3**, **DT-M**, **DP-P** and **DT-P**.

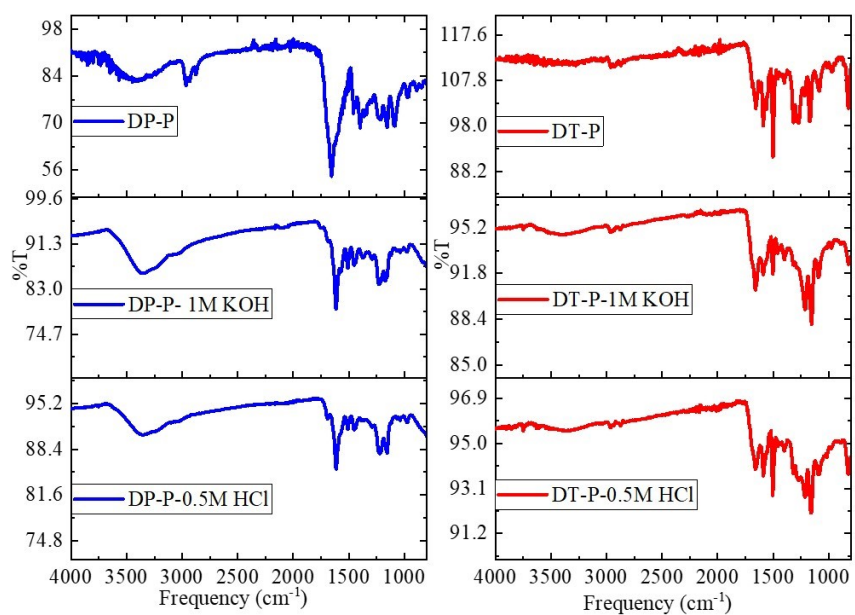


Fig S 2: FTIR spectra of **DP-P** and **DT-P** polymers taken after soaking the polymers for 5 days in 1M KOH and 0.5M HCl.

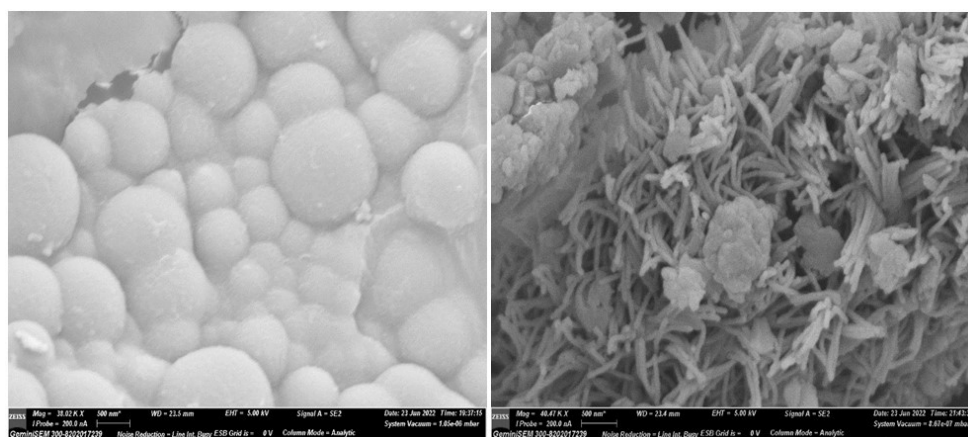


Fig S 3: FE-SEM of the **DT-P**(Left) and **DP-P**(Right).

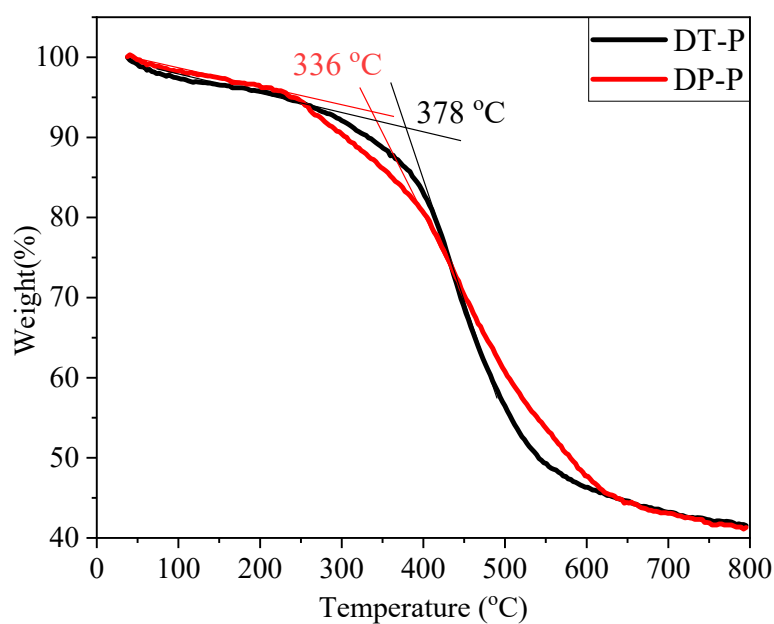


Fig S 4: TGA of **DP-P** and **DT-P** polymers.

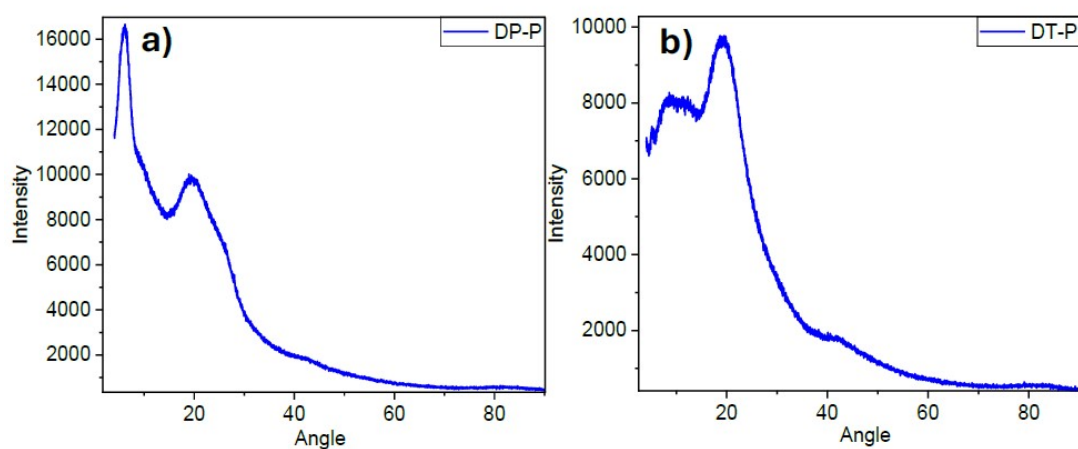


Fig S 5: Powder XRD of **DP-P** and **DT-P** polymers.

XPS analysis: The synthesized polymers were analysed using XPS to investigate the different types of atoms present in the polymers. The survey scan spectra of **DP-P** and **DT-P** showed peaks at 533, 402, and 286 eV, and 532, 403, and 285 eV, respectively, corresponding to the 1s orbitals of O, N, and C atoms (Fig. S6).

In addition to the survey scan spectra, high-resolution spectra of individual atoms were obtained. For **DP-P**, the N(1s) peak at 399.7 eV was assigned to the N-C bond of the DPP ring,

and the O(1s) peak at 531.4 eV corresponded to the O=C group of the DPP ring. The C(1s) spectrum revealed three distinct peaks: 292.1 eV (C=O), 287.6 eV (C-O-C), and 284.5 eV (C-C)(Fig S7), indicating various types of carbon atoms in the polymer backbone.

Similarly, the high-resolution spectra of **DT-P** showed an N(1s) peak at 399.6 eV, attributed to the DPP ring, and an O(1s) peak at 531.4 eV, corresponding to the O=C group of the DPP ring. The C(1s) spectrum exhibited three peaks at 284.4 eV (C-C), 287.5 eV (C-N), and 292.2 eV (C=O) (Fig S7). The presence of these characteristic peaks confirms the incorporation of the DPP core into the polymer backbone.

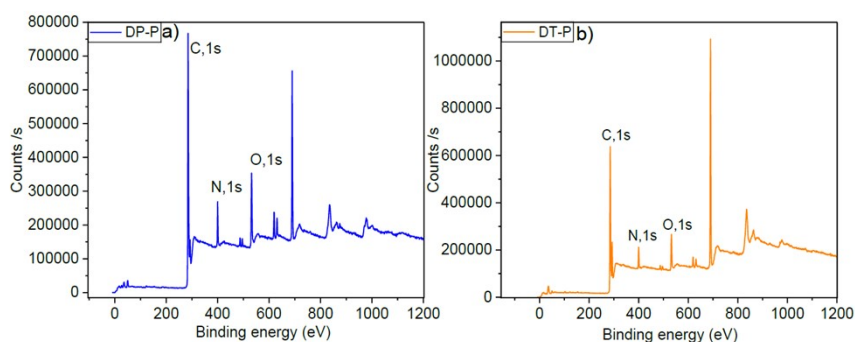


Fig S 6: XPS survey scan spectra of DP-P and DT-P polymers.

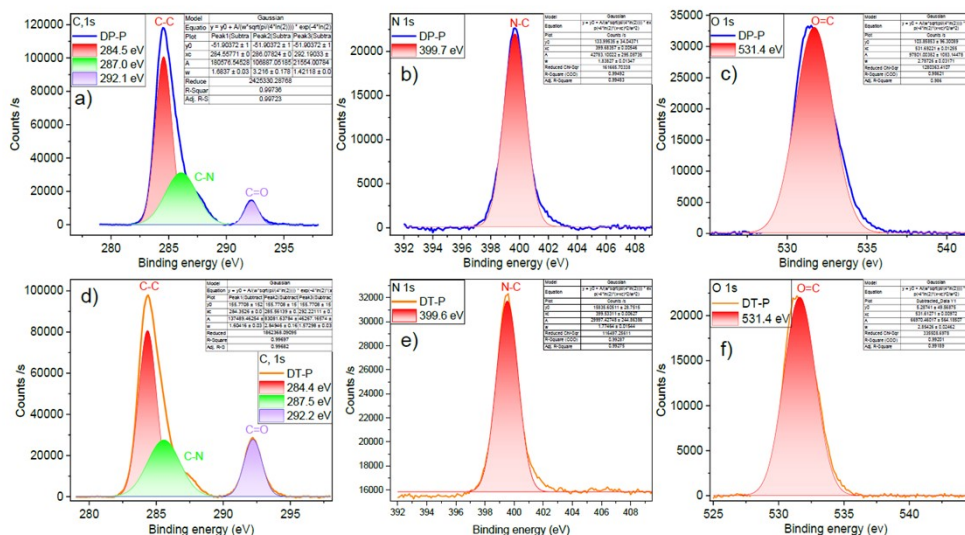


Fig S 7: High resolution XPS spectra of C 1s (a), N 1s (b), O 1s (c) of **DP-P** and C 1s (d), N 1s (e), O 1s (f) of **DT-P**.

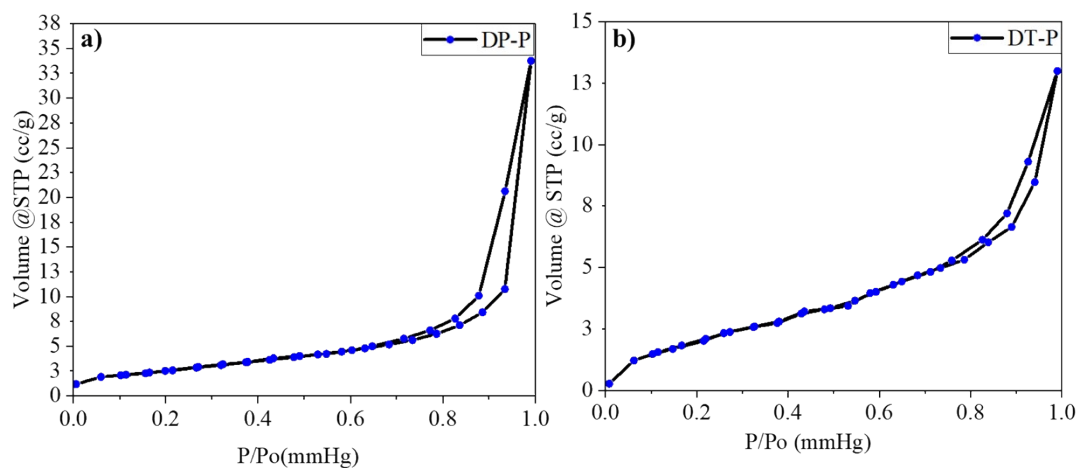


Fig S 8: BET adsorption isotherms of **DP-P** and **DT-P** polymers.

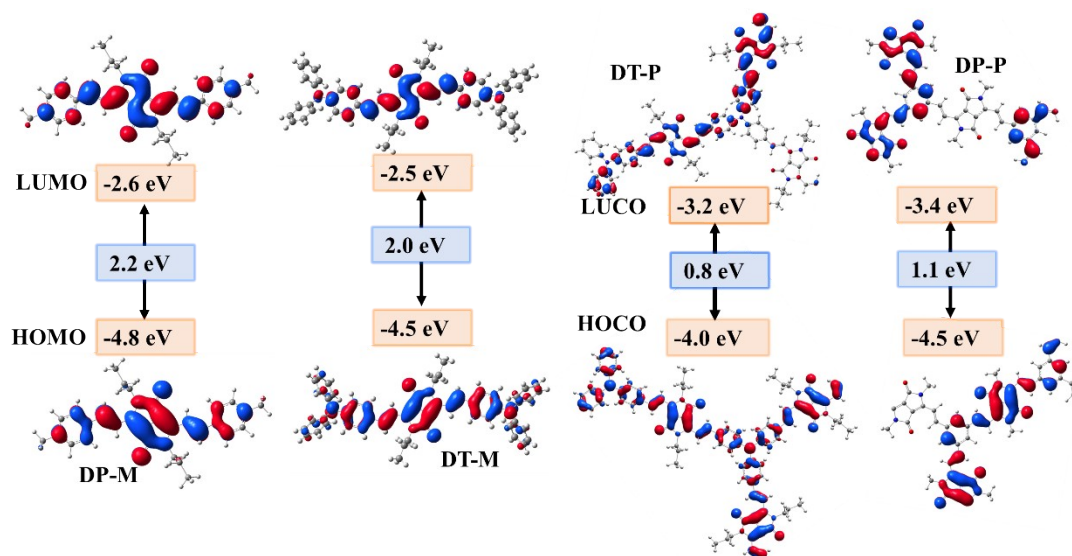


Fig S 9: The DFT computed frontier molecular orbitals of model compounds **DP-M** and **DT-M** (left side) and polymers **DP-P** and **DT-P** (right side) by using B3LYP-631G(d) basis set method.

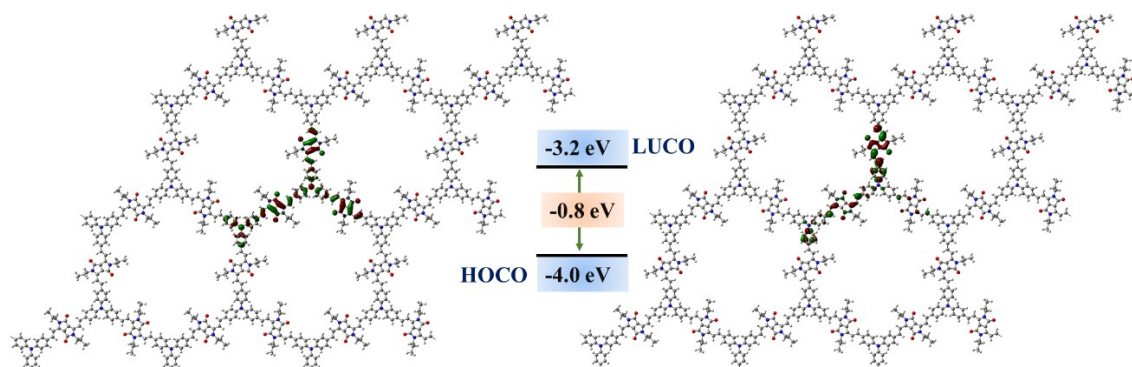


Fig S 10: DFT computed HOCO and LUCO of **DT-P** polymer.

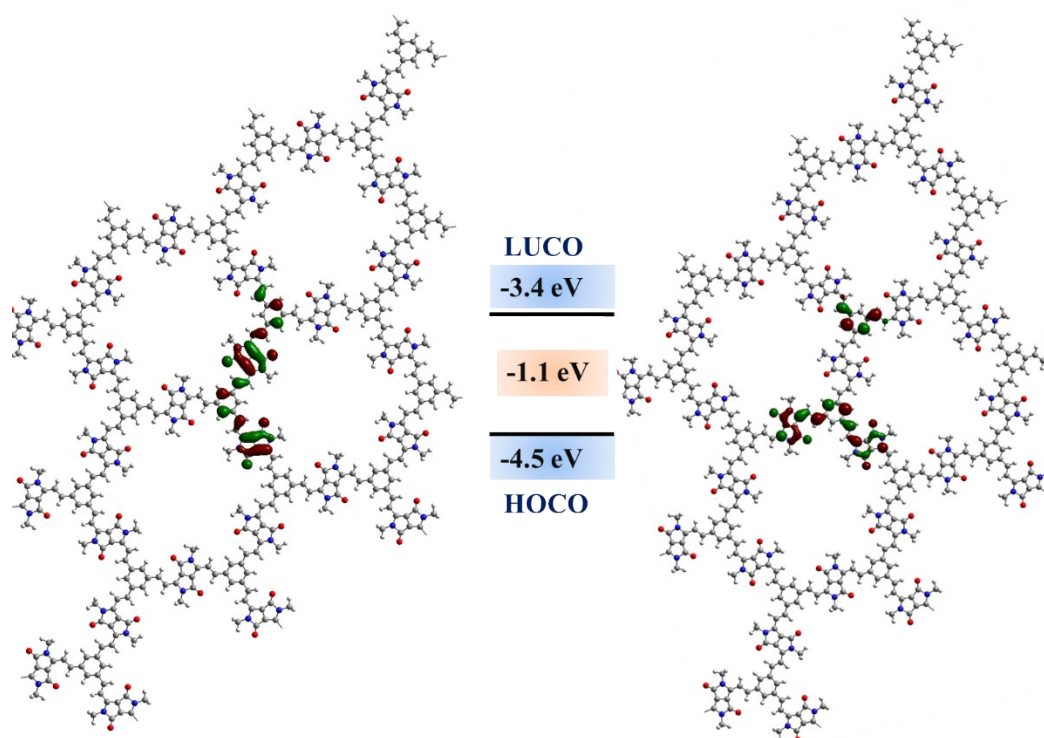
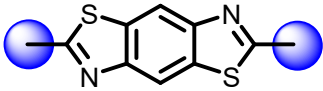
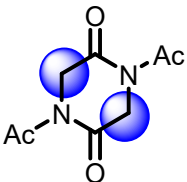
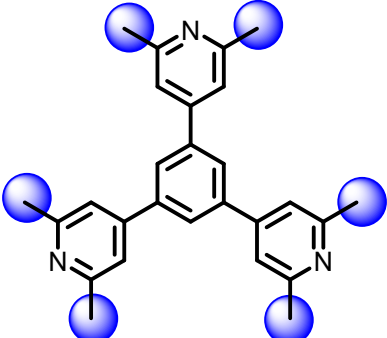
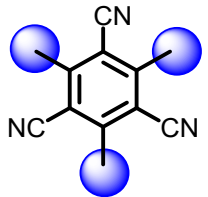
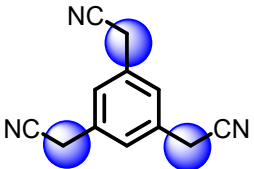
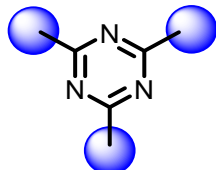
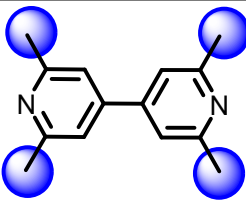
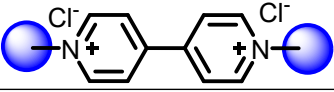
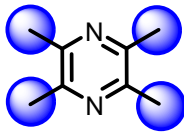
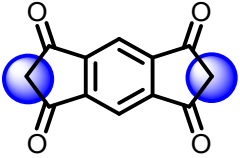
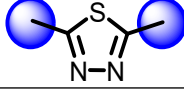
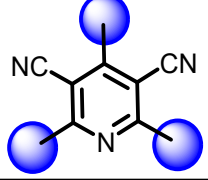
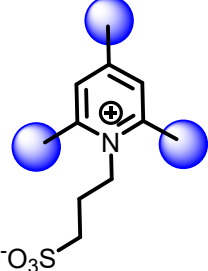


Fig S 11: DFT computed HOCO and LUCO of **DP-P** polymer.

Table S 1: Reported active methylene building block.

Sl No.	Active methylene building blocks	References
1		<i>ACS Catal.</i> 2023 , <i>13</i> , 1089–1096. ⁴
3		<i>J. Mater. Chem. C.</i> 2024 , <i>12</i> , 110-117. ⁵
4		<i>J. Am. Chem. Soc.</i> 2023 , <i>145</i> , 16704–16710. ⁶

5		<i>J. Am. Chem. Soc.</i> 2020 , <i>142</i> , 11893–1190. ⁷
6		<i>Adv. Funct. Mater.</i> 2017 , <i>27</i> , 1700233(1-9). ⁸
7		<i>Angew. Chem.</i> 2019 , <i>131</i> , 15007–15012. ⁹
8		<i>J. Am. Chem. Soc.</i> 2022 , <i>144</i> , 3653–3659. ¹⁰
9		<i>J. Am. Chem. Soc.</i> 2023 , <i>145</i> , 21284–21292. ¹¹
10		<i>J. Am. Chem. Soc.</i> 2023 , <i>145</i> , 21483–21490. ¹²
11		<i>J. Am. Chem. Soc.</i> 2023 , <i>145</i> , 1022–1030. ¹³
12		<i>J. Am. Chem. Soc.</i> 2024 , <i>146</i> , 1318–1325. ¹⁴
13		<i>Angew. Chem. Int. Ed.</i> 2019 , <i>58</i> , 12065–12069. ¹⁵
14		<i>J. Am. Chem. Soc.</i> 2023 , <i>145</i> , 25222–25232. ¹⁶

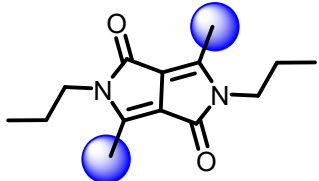
15		Our work
----	---	----------

Table S 2: Absorption of the reported DPP integrated 2D polymers.

Sl no.	Polymer	Absorption $\lambda(\text{nm})$	Reference
1	DPP2-HHTP-COF	700 nm	<i>Chem.Mater.</i> 2019,31,2707-2712. ¹⁶
2	Py-DPP-COF@CNT	-	<i>ACS Energy Lett.</i> 2021,6,3053-3063. ¹⁷
3	DPP-TPP-COF DPP-TBB-COF	500-800 nm	<i>Small.</i> 2024, 2402993(1-10). ¹⁸
4	Uni-DPP-PPN Uni-DPP-PPN-F ⁻	200-600 nm	<i>J. Mater.Chem. C.</i> 2018, 6, 3961-3967. ¹⁹
5	DT-P DP-P	Up to 1200 nm	Our work

Table S 3: Electrical conductivity of the reported 2D polymers.

Sl no.	Polymer	Electrical conductivity of pristine sample (Two probe) (S m^{-1})	Electrical conductivity of the doped sample (Two probe) (S m^{-1})	References
2	TTF-Ph-COF TTF-Py-COF	10^{-3} 10^{-4}	-	<i>Chem. Eur. J.</i> 2014 , 20, 14608 – 14613. ²⁰
3	1S 1Se 1Te	3.7×10^{-8} 8.4×10^{-7} 1.3×10^{-5}	-	<i>Chem. Mater.</i> 2015 , 27, 5487–5490. ²¹
7	3D-TTF COFs	-	1.4	<i>J. Am. Chem. Soc.</i> 2019 , 141, 13324–13329. ²²
8	TANG COF	5×10^{-12} (inplane) 1.6×10^{-5} (out of plane)	2×10^{-1} (inplane) 1.5×10^{-1} (out of plane)	<i>J. Am. Chem. Soc.</i> 2020 , 142, 2155–2160. ²³
9	c-HBC-COF	10^{-8}	3.0×10^{-5}	<i>J. Am. Chem. Soc.</i> 2022 , 144, 5042–5050. ²⁴

11	TTF-DMTA	-	$1.7 \cdot 10^{-4}$	<i>ACS Appl. Mater. Interfaces.</i> 2020 , <i>12</i> , 19054–19061. ²⁵
12	CTPA STPA	$\sim 10^{-7}$	0.1 $5 \cdot 10^{-2}$	<i>Chem. Commun.</i> , 2023 , <i>59</i> , 8846–8849. ²⁶
13	nQ1 Q1	$\sim 10^{-7}$	$2 \cdot 10^{-3}$ $8 \cdot 10^{-3}$	<i>J. Mater. Chem. C</i> , 2024 , <i>12</i> , 110–117. ⁵
14	DT-P	$3.4 \cdot 10^{-3}$	$1.92 \cdot 10^{-1}$	Our work

General procedure for supercapacitance testing of the DP-P and DT-P polymers

A 5 mm-diameter glassy carbon disk electrode (Pine Research Instrumentation, US) was coated with the ink containing electrode active materials. Three formulations were investigated: a bare polymer, a polymer with carbon black, and a polymer with carbon black and graphene oxide. A slurry was prepared by dispersing 10 mg of polymer and 1 mL of Nafion (5 wt%; Aldrich Canada) in EtOH (1:4; a stock solution was prepared from 2 mL of 5 wt% Nafion + 8 mL of ethanol = 10 mL total) and then sonicating for 0.5 h. A 10 μ L was pipetted onto the tip of the electrode, which was then dried in air for 10 min before use.

A slurry with carbon black and graphene oxide was prepared by dispersing 10 mg of polymer and 2 mg of carbon black and graphene oxide in the same mixture of solvents.

A glassy carbon disk electrode was polished with 0.05-micron Al₂O₃ and rinsed in water and absolute ethanol with sonication.

All electrochemical tests were carried out in a 3-electrode electrochemical cell with an Ag/AgCl reference electrode ($E = 0.221$ V), a platinum wire counter electrode, and 1 M KOH (Aldrich, Canada) electrolyte. The electrolyte was purged with nitrogen gas for 30 min to remove dissolved oxygen, and a gas blanket was kept above the solution during all electrochemical tests. A potentiostat model CHI 760e (CH Instruments Inc., United States) was used for all electrochemical tests related to testing materials as potential capacitor electrodes. Cyclic voltammograms at various potential scan rates (5-100 mV/sec) were recorded and used

to quantify a specific (gravimetric) capacitance (C_s) and the diffusion coefficient (D) of the ionic species from the electrolyte that compensates for the charge change during the polymer redox activity. As such, quantifying the specific gravimetric capacitance (C_s) and the results of this analysis are projected in **Table 1**. The area bound by the CV is related to C_s (F/g) by the **Eqn. S1**, where $i(E)$ is the instantaneous current of the CV, v is the scan rate (V/s), V is the potential window (V), and m is the mass of active material (g). The mass of polymers cast on a glassy carbon disk is taken as a mass of active material.

$$C_s = \frac{i(E)dE}{2vmV} \quad \text{Eqn. S1}$$

Diffusion coefficients (D) are helpful in studying the rate of charge compensation by ionic species present in the electrolyte during the redox activity of the polymer. Through the Randles-Sevcik equation (**Eqn. S2**), a linear function of peak current (i_p) vs. the square root of the scan rate (v) is obtained (**Fig. S13-17**). The plot of variable scan rates or the samples can be found in (**Fig. S11-12**).

$$i_p = 0.4463nFAC\left(\frac{nFDv}{RT}\right)^{1/2} \quad \text{Eqn. S2}$$

D also relies upon these parameters: n = no. of electrons transferred, A = electrode area (cm²), F = Faraday's constant (C/mol), C = electrolyte concentration (M), R = gas constant (J/mol*K), and T = temperature (K).

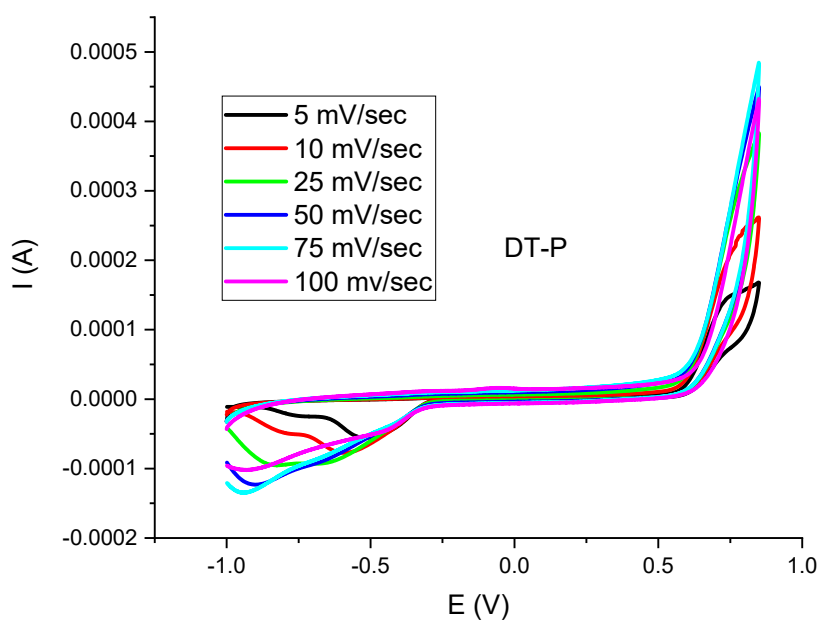


Fig S 12: Cyclic voltammograms of bare **DT-P** polymer in 1 KOH recorded at various potential scan rates: 5-100 mV/sec.

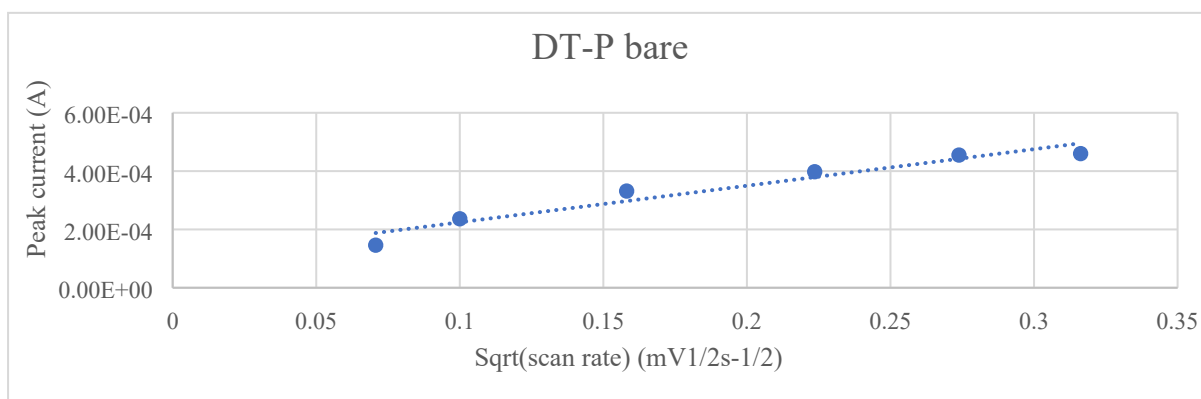


Fig S 13: A reduction peak current vs. square root of potential scan rate built based on cyclic voltammograms in Fig. S11 for bare **DT-P** polymer.

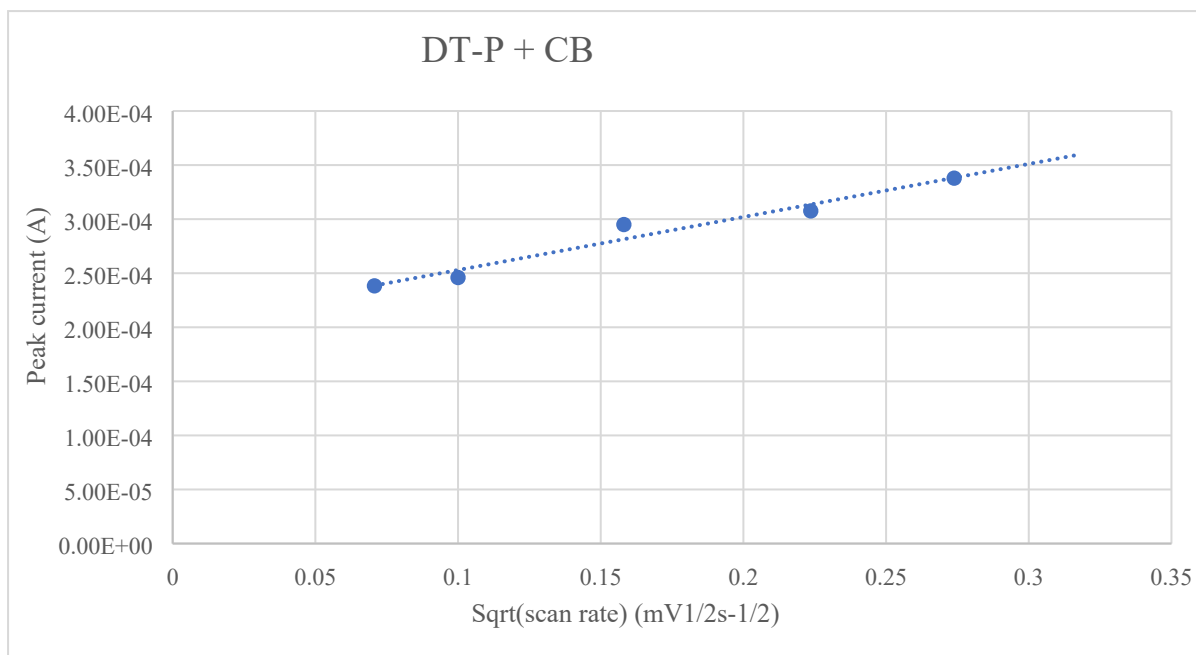


Fig S 14: A reduction peak current vs. square root of potential scan rate built based on cyclic voltammograms for **DT-P** + CB (carbon black).

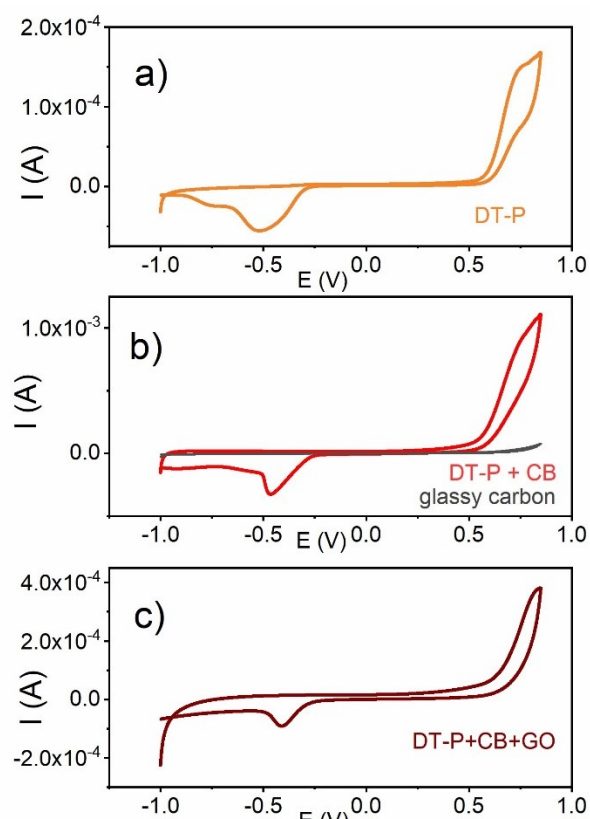


Fig S 15: The cyclic voltammogram of **DT-P** polymer (a); **DT-P** + carbon black (CB) (b); **DT-P** + CB + graphene oxide (GO) (c).

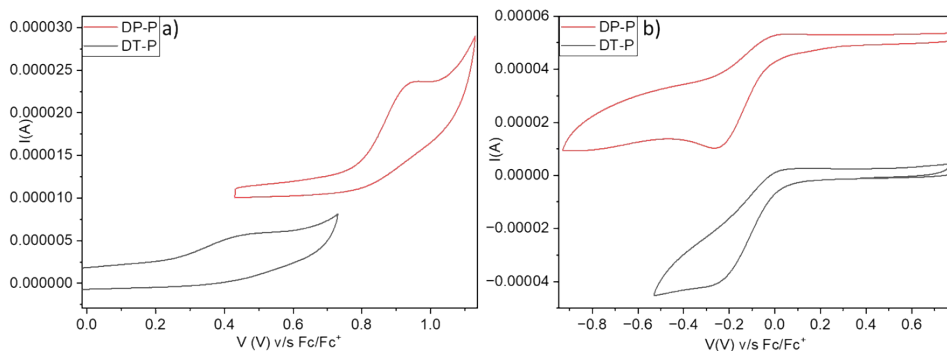


Fig S 16: The cyclic voltammogram of DP-P and DT-P polymers measured by using dichloromethane as solvent and tetrabutylammonium chloride as an electrolyte at 20 mV/s scan rate.

Table S 4: Specific capacitance (C_s ; F/g) and diffusion coefficient (D ; cm^2/s) for bare polymers and their mixture with carbon black (CB) and graphene oxide (GO).

Sample	C_s (F/g)	D (cm^2/s)
DP-P ^a	11	1.75×10^{-16}
DP-P+CB ^b	21	1.89×10^{-15}
DP-P+CB+GO ^c	41	4.33×10^{-16}
DT-P ^a	18	5.16×10^{-16}
DT-P+CB ^b	11	8.96×10^{-17}
DT-P+CB+GO ^c	70	-
CB+GO	13	-

^a – pure polymer; ^b – polymer + carbon black (CB); ^c – polymer + CB + graphene oxide (GO)

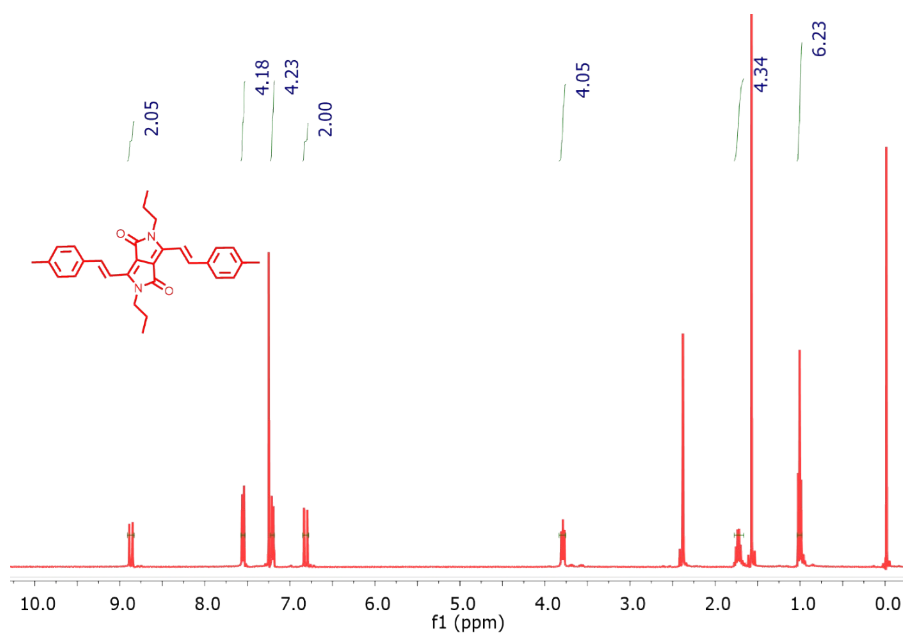


Fig S 17: ^1H NMR of DP-M.

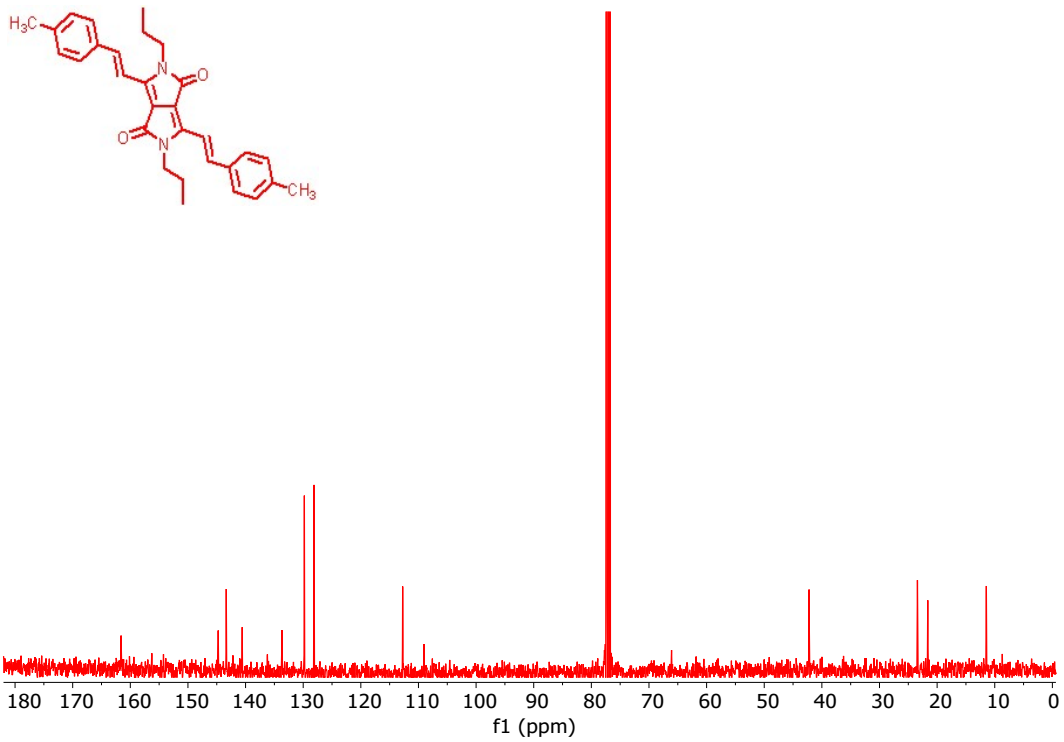


Fig S 18: ¹³C NMR of DP-M.

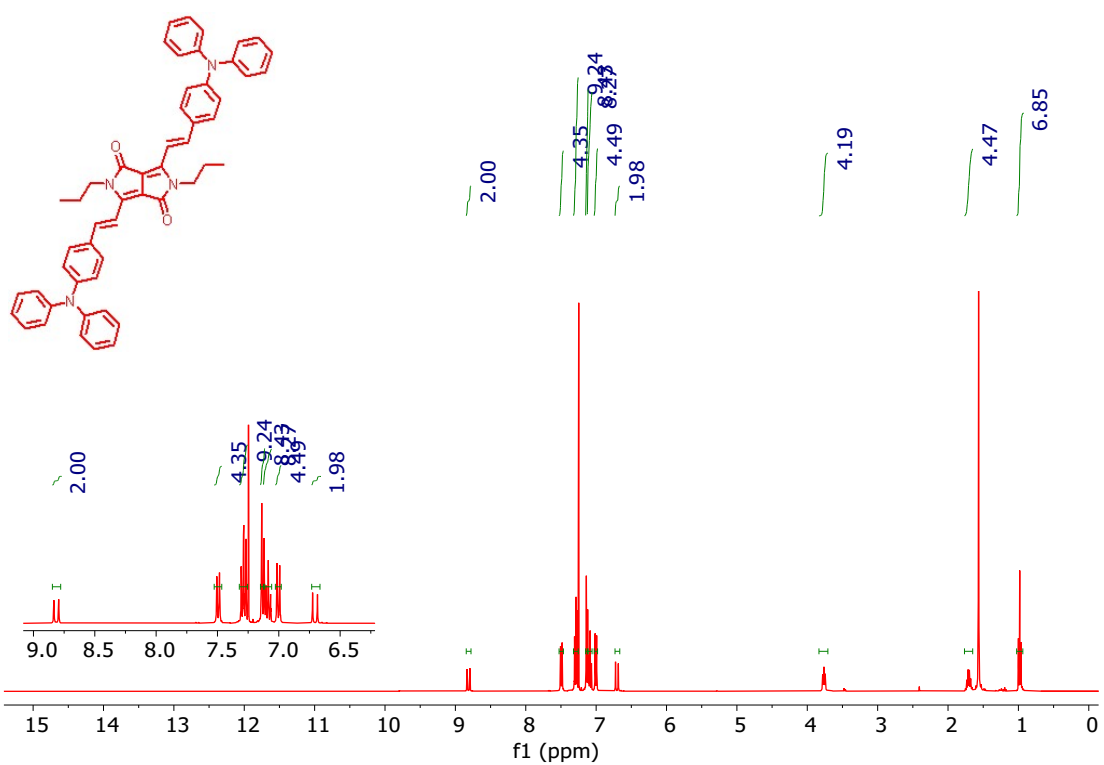


Fig S 19: ¹H NMR of DT-M.

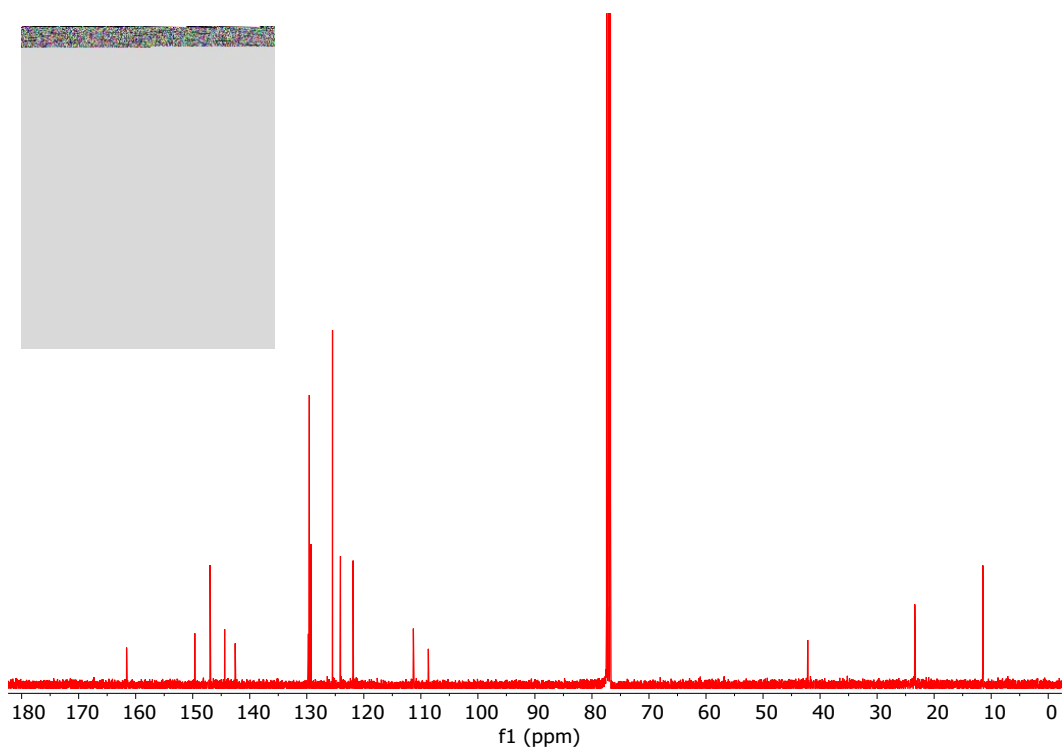


Fig S 20: ^{13}C NMR of DT-M.

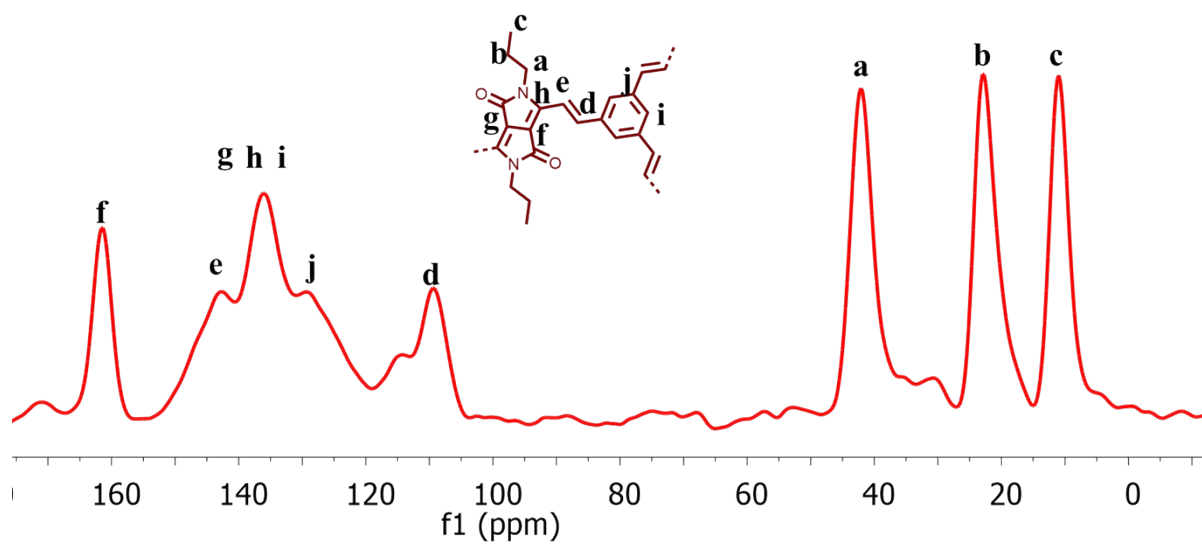


Fig S 21: ^{13}C -CPMAS of DP-P.

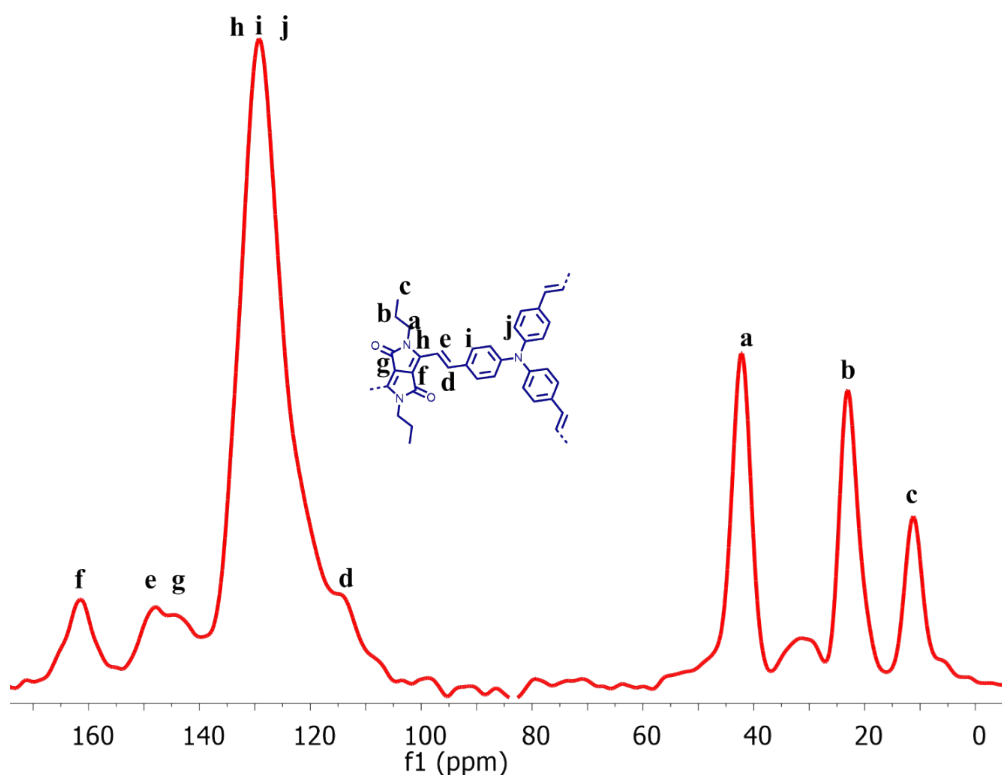


Fig S 22: ^{13}C -CPMAS of DT-P.

References:

- 1 T. Kunde, E. Nieland, H. V. Schröder, C. A. Schalley and B. M. Schmidt, *Chem. Commun.*, 2020, **56**, 4761–4764.
- 2 C. Li, W. Yang, W. Zhou, M. Zhang, R. Xue, M. Li and Z. Cheng, *New J. Chem.*, 2016, **40**, 8837–8845.
- 3 Vinutha K. Venkatareddy and M. Rajeswara Rao, *RSC Adv.*, 2024, **14**, 10017–10023.
- 4 S. Li, R. Ma, S. Xu, T. Zheng, H. Wang, G. Fu, H. Yang, Y. Hou, Z. Liao, B. Wu, X. Feng, L.Z. Wu, X.B. Li and T. Zhang, *ACS Catal.*, 2023, **13**, 1089–1096.
- 5 A. R. K and M. Rajeswara Rao, *J. Mater. Chem. C*, 2023, **12**, 110–117.
- 6 Z. Zhang, S. Bi, F. Meng, X. Li, M. Li, K. Mou, D. Wu and F. Zhang, *J. Am. Chem. Soc.*, 2023, **145**, 16704–16710.
- 7 S. Bi, P. Thiruvengadam, S. Wei, W. Zhang, F. Zhang, L. Gao, J. Xu, D. Wu, J. S. Chen and F. Zhang, *J. Am. Chem. Soc.*, 2020, **142**, 11893–11900.
- 8 A. Yassin, M. Trunk, F. Czerny, P. Fayon, A. Trewin, J. Schmidt and A. Thomas, *Adv. Funct. Mater.*, 2017, **27**, 1700233.
- 9 J. M. Chen, H. Duan, Y. Kong, B. Tian, G.-H. Ning and D. Li, *Energy Fuels*, 2022, **36**, 5998–6004.
- 10 S. Bi, F. Meng, D. Wu and F. Zhang, *J. Am. Chem. Soc.*, 2022, **144**, 3653–3659.
- 11 X. N. Feng, Y. Yang, X. Cao, T. Wang, D.-M. Kong, X. B. Yin, B. Li and X.-H. Bu, *J. Am. Chem. Soc.*, 2023, **145**, 21284–21292.
- 12 Z. Wang, Y. Zhang, E. Lin, S. Geng, M. Wang, J. Liu, Y. Chen, P. Cheng and Z. Zhang, *J. Am. Chem. Soc.*, 2023, **145**, 21483–21490.

- 13 X. Xu, S. Zhang, K. Xu, H. Chen, X. Fan and N. Huang, *J. Am. Chem. Soc.*, 2023, **145**, 1022–1030.
- 14 G. Fu, D. Yang, S. Xu, S. Li, Y. Zhao, H. Yang, D. Wu, P. S. Petkov, Z.-A. Lan, X. Wang and T. Zhang, *J. Am. Chem. Soc.*, 2024, **146**, 1318–1325.
- 15 J. Xu, Y. He, S. Bi, M. Wang, P. Yang, D. Wu, J. Wang and F. Zhang, *Angew Chem. Int. Ed.*, 2019, **58**, 12065–12069.
- 16 S. Rager, A. C. Jakowetz, B. Gole, F. Beuerle, D. D. Medina and T. Bein, *Chem. Mater.*, 2019, **31**, 2707–2712.
- 17 J. Xu, W. Tang, C. Yang, I. Manke, N. Chen, F. Lai, T. Xu, S. An, H. Liu, Z. Zhang, Y. Cao, N. Wang, S. Zhao, D. Niu and R. Chen, *ACS Energy Lett.*, 2021, **6**, 3053–3062.
- 18 L. Luo, C. Li, Y. Wang, P. Chen, Z. Zhou, T. Chen, K. Wu, S.Y. Ding, L. Tan, J. Wang, and X. Shao, *Small*, 2024, **15**, 2402993.
- 19 S. Bi, Y. Li, S. Zhang, J. Hu, L. Wang and H. Liu, *J. Mater. Chem. C*, 2018, **6**, 3961–3967.
- 20 S. Jin, T. Sakurai, T. Kowalczyk, S. Dalapati, F. Xu, H. Wei, X. Chen, J. Gao, S. Seki, S. Irle and D. Jiang, *Chemistry A European J*, 2014, **20**, 14608–14613.
- 21 S. Duhović and M. Dincă, *Chem. Mater.*, 2015, **27**, 5487–5490.
- 22 H. Li, J. Chang, S. Li, X. Gun, D. Li, C. Li, L. Tang, M. Xue, Y. Yan, V. Valtchev and S. Qiu, *J. Am. Chem. Soc.* 2019, **141**, 13324–13329.
- 23 V. Lakshmi, C.H. Liu, M. Rajeswara Rao, Y. Chen, Y. Fang, A. Dadvand, E. Hamzehpoor, Y. Sakai-Otsuka, R. S. Stein and D. F. Perepichka, *J. Am. Chem. Soc.*, 2020, **142**, 2155–2160.
- 24 G. Xing, W. Zheng, L. Gao, T. Zhang, X. Wu, S. Fu, X. Song, Z. Zhao, S. Osella, M. Martínez-Abadía, H. I. Wang, J. Cai, A. Mateo-Alonso and L. Chen, *J. Am. Chem. Soc.*, 2022, **144**, 5042–5050.
- 25 S. Cai, B. Sun, X. Li, Y. Yan, A. Navarro, A. Garzón-Ruiz, H. Mao, R. Chatterjee, J. Yano, C. Zhu, J. A. Reimer, S. Zheng, J. Fan, W. Zhang and Y. Liu, *ACS Appl. Mater. Interfaces*, 2020, **12**, 19054–19061.
- 26 S. Enoch, A. B. Nipate, V. Lakshmi and M. Rajeswara Rao, *Chem. Commun.*, 2023, **59**, 8846–8849.